Materials Letters 355 (2024) 135575

Contents lists available at ScienceDirect

Materials Letters

journal homepage: www.elsevier.com/locate/matlet

Salicylic acid-loaded gelatin methacryloyl (GELMA) microneedles as a potential drug delivery system in plant diseases

Ayse Gulcan Ipek, Huseyin Berkay Ozarici, Ugur Sayil, Hatice Karabulut, Songul Ulag *, Oguzhan Gunduz *

Center for Nanotechnology & Biomaterials Application and Research (NBUAM), Marmara University, Istanbul, Turkey

ARTICLE INFO

Keywords:
Biomaterials
Gelatin methacryloyl
Microneedle
Salicylic acid
3D printing

ABSTRACT

In this research, gelatin methacryloyl (GELMA) was used as a matrix material to obtain microneedles (MNs), and salicylic acid (SA) was added to this solution to investigate the release behavior of the SA from the needles. The scanning electron microscope (SEM) images showed that the uniform conical shape of MN structures was observed. According to the compression test results, MNs could penetrate deeply into plant tissue without breaking due to their practical toughness. The release behavior of the SA was carried out *in vitro* conditions and completed in 24 h.

1. Introduction

Plants are commonly used in industry. People have been obtaining and utilising their oil, fruit, and leaves, turning them into useful products for many areas such as cosmetics, food, pharmaceuticals, etc. These evolutions have made plants more desired substrates, especially in the food industry [1]. This industry has been developed over the years since humanity started to evolve. However, due to the environment, plants are also able to get the disease. Each disease may react differently to changes in CO_2 concentrations, temperature, and water availability, which can have positive, neutral, or adverse effects on disease development [2]. These diseases can also be caused by bacteria, fungi, or viruses, and they can affect plants directly or indirectly. By defeating the immune system of the plants they transmit, they create situations that can result in death [3]. Physiologically; colour change, little spots, dryness on the leaves, and broken leaves can be observed in their phenotypes [4]. Preventing disease using pesticides can be an option, but in the long term, chemicals within pesticides will decrease the efficiency of soil and crops [5]. On infected plants, the colour change may occur on leaves as spots, dryness of the spot, and results in the break [6]. MNs could be a good solution for the treatment of plants locally. By applying on the skin, MNs could be an advantage for local drug delivery and the loss of the drug in amount and efficiency [7]. The same situation can also be considered for plants. Using drug-loaded MNs not only treats locally but also decreases the use of pesticides in high amounts and prevents the disadvantages that could have occurred to human health and crops. They also have almost non-side effects and can be easily applied [8]. The MN system is an effective method for delivering medicinal molecules with larger masses (above 500 Da) and different polarities compared to the other traditional techniques [9]. In this study, for the first time, SA-loaded GELMA MNs were produced and their characterizations were examined for the purpose of local and controlled drug delivery on plant diseases. This will be novel study which can open a new perspective about using of drug loaded MNs in plant diseases. GELMA has biocompatibility, tunable mechanical properties, and capacity to support cell growth [10]. The major function of SA is to establish systemic acquired resistance (SAR) that helps plants resist to variety of pathogens [11]. In the literature, amoxicillin-loaded GELMA MNs were fabricated for transdermal drug delivery [12].

2. Materials & method

GELMA was obtained from Collagen ArGe company (Turkey). The phosphate-buffered saline (PBS, pH of 7.4) was purchased from Chem-Bio, Turkey. The SA (MW: 138 g/mol) was acquired from Sigma Aldrich (USA). The lithium phenyl-2,4,6-trimethyl-benzoyl phosphinate (LAP) (95 % purity, MW: 294.21 g/mol) was obtained from Sigma Aldrich (USA). The 1 mL PBS solution was measured and transferred into a beaker for GELMA solution preparation. The beaker was put on the magnetic stirrer at 140 rpm, 30 °C. Gradually, 0.1 g of GELMA powder was added and mixed on the stirrer. Then, 20 mg of SA was added and mixed for 5 min. Then 2.5 mg of LAP was added and stirred for 5 min.

* Corresponding authors.
E-mail addresses: songul.ulag@marmara.edu.tr (S. Ulag), ucemogu@ucl.ac.uk (O. Gunduz).

https://doi.org/10.1016/j.matlet.2023.135575
Received 22 June 2023; Received in revised form 10 October 2023; Accepted 12 November 2023
Available online 13 November 2023

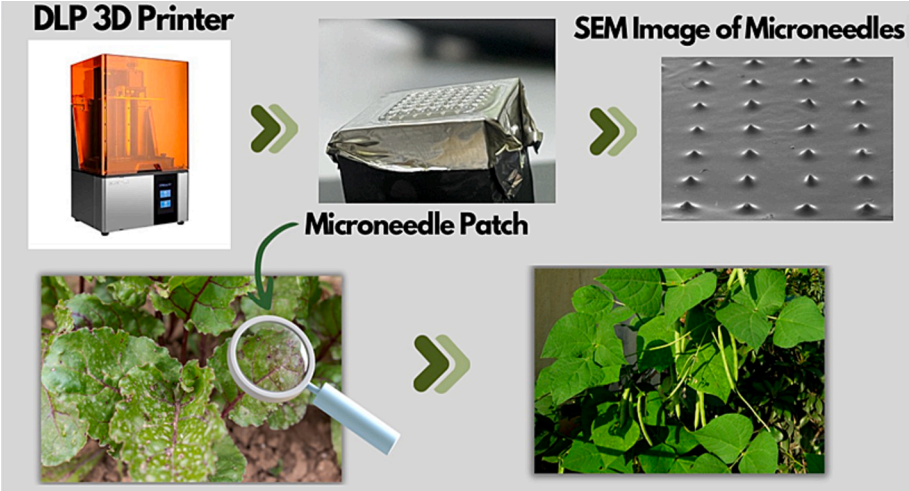

Fig. 1. The fabrication steps of the study.

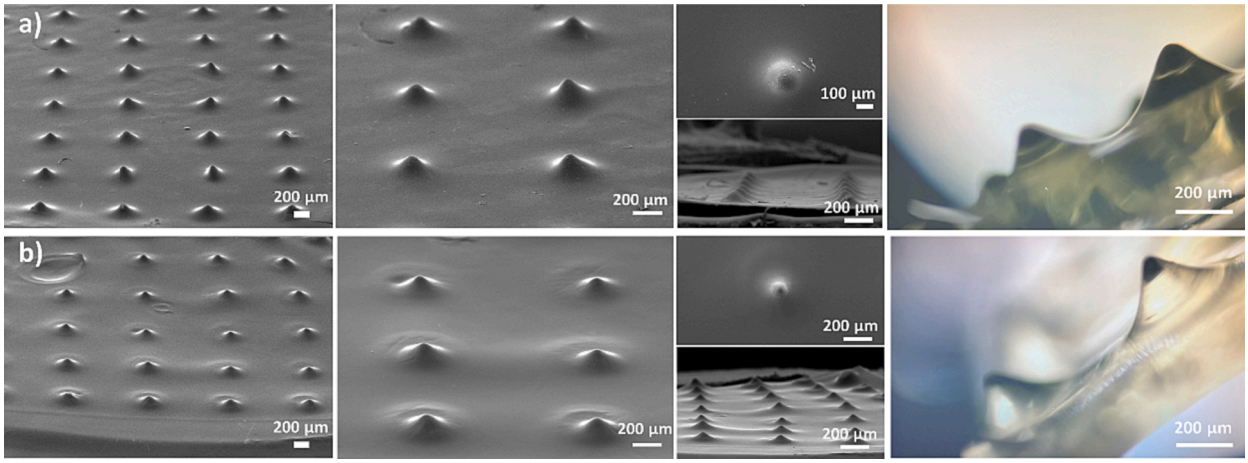

Fig. 2. The SEM and optical images of GELMA (a) and SA-loaded GELMA (b) MNs.

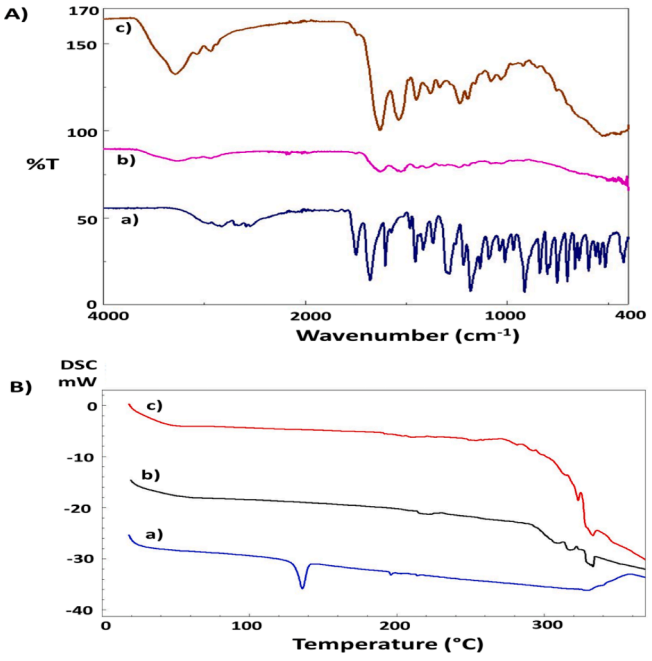

Fig. 3. FTIR analysis of the pristine SA (A, a), GELMA (A, b), and SA-loaded GELMA (A, c) MNs; DSC curves of the pristine SA (B, a), GELMA (B, b), SA-loaded GELMA (B, c) MNs.

The Phrozen Sonic Mini 8 K 3D printer was used to prepare MNs. The bottom exposure and normal exposure were both set to 90.000 s to ensure suitable solidification and cure of the microneedle layers. The incorporation of 6 bottom layers improves MNs' stability and adhesion. The design of MNs was created on a square base with dimensions of 10 mm width and 1.50 mm depth in Solidworks. The design comprised of 49 needles with a 7x7 configuration. Each needle exhibited a height of 0.95 mm, with uniform spacing at intervals of 1.40 mm. Then transferred into the printer's software after being exported in an STL format. The SA-loaded GELMA solution was added to the printer's reservoir and the UV light was turned on for slow layer-by-layer solidification. After obtaining the MNs (Fig. 1), the physicochemical properties of the MNs were investigated with fourier transform infrared spectroscopy (FTIR, 4700 Jasco, Japan) with a resolution of 4 cm^{-1}. The SEM (MA-EVO 10, ZEISS, Germany) was used to examine the morphologies of MNs. They were vacuum-coated with gold for 60 s prior to analysis. The thermal properties of the needles were investigated with DSC (DSC-6O Plus, Shimadzu) with 25–350 °C temperature range and 10 °C/min heating rate. The mechanical properties of the MNs were carried out with a compression testing machine (EZ-LX, Shimadzu, Japan). They were positioned 2 mm apart on a stainless steel plate, and an axial force perpendicular to the axis of the MNs was applied at a constant rate of 0.1 mm/min. The absorbance values of 5 distinct drug concentrations (0.2, 0.4, 0.6, 0.8, and 1 mL) were measured to calculate the calibration curve of the SA. The prepared MNs were put into eppendorf tubes with 1 mL of PBS solution. At 37 °C and 300 rpm, the tubes were placed in a thermal

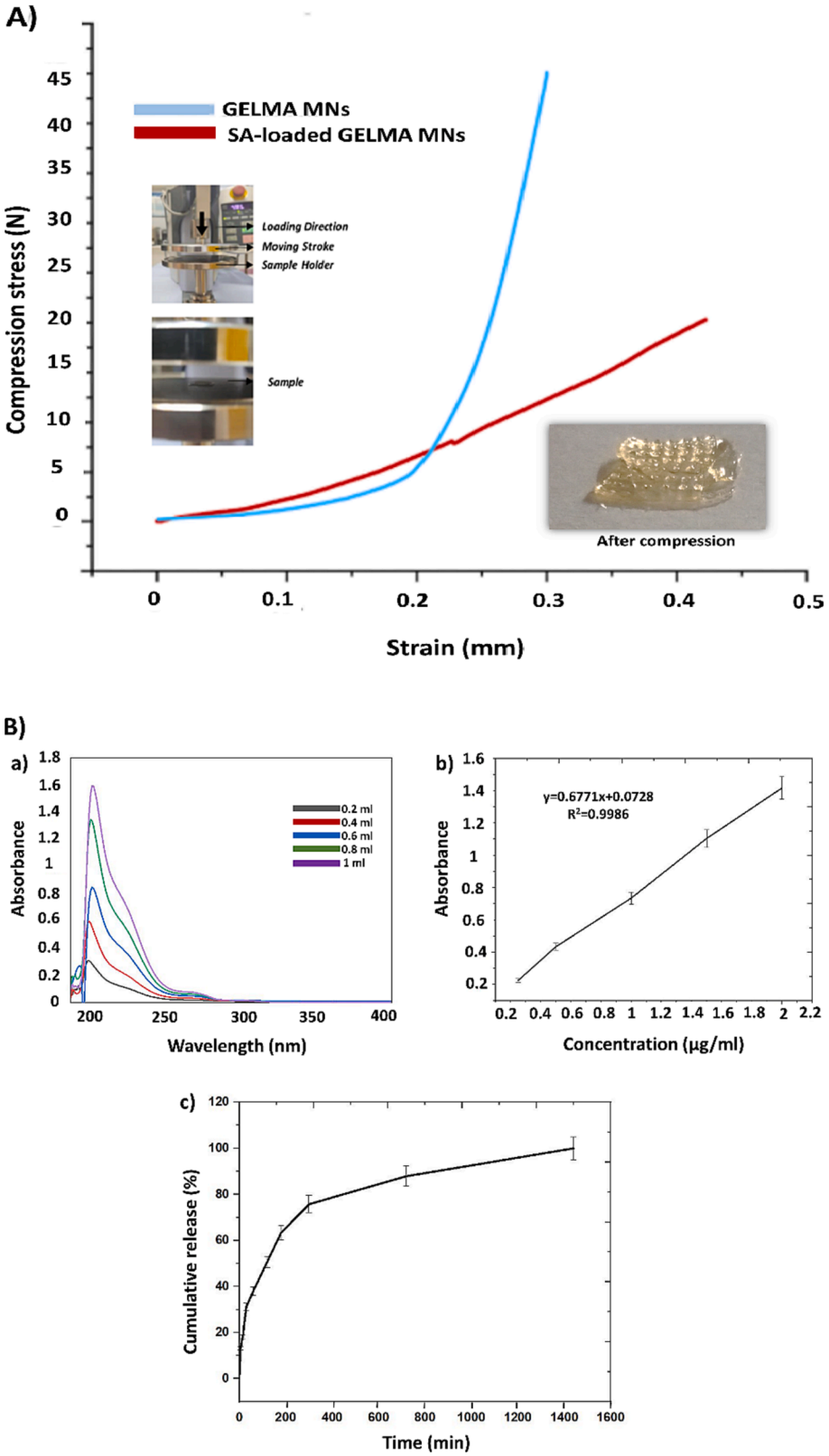

Fig. 4. The compression test results of GELMA and SA-loaded GELMA MNs (A), the calibration curve of SA (B, a), absorbance graph (B, b), and cumulative release graph of the SA (B, c).

shaker. UV–visible spectrophotometer measurements were made at different time intervals (5, 15, 30, 60, 120, 180, 300, 720, and 1440 min), and samples were refreshed with PBS after each measurement. The experiments was performed with three replicates.

3. Results & discussions

The SEM images of MNs are shown in Fig. 2. The produced MNs had quite normal and uniform morphology, a visible sharp tip, and no air bubbles or agglomeration in their structure. The addition of SA didn't cause big differences in the structure of the MNs, and smaller MNs were obtained. The FTIR graphs are shown in Fig. 3 (A). The peaks between 2827.13 cm^{-1} and 1749.12 cm^{-1} were related to the presence of C-H and C═O groups for SA. Another characteristic peak of SA was observed between 1679.69 cm^{-1} and 1286.29 cm^{-1} (stretching vibrations of acidic hydrogen of the phenol hydroxyl, CH═CH_2, and C═C groups) [13]. GELMA had main peaks at 3286.11 cm^{-1} (O-H and N-H stretching vibrations), 1637.27 cm^{-1} (C═O stretching), 1542.77 cm^{-1} (N-H bending coupled to C-H stretching), and 1238.08 cm^{-1} (C-N stretching and N-H bending) [14]. The addition of SA to GELMA resulted in some shift in FTIR peaks, proving the homogeneity within the MNs [15]. The thermal analysis results are shown in Fig. 3 (B). The MNs resulted in a weak peak at approximately 220 ℃, which is correlated with the melting point of the polymer [16]. However, adding the SA to the GELMA changed the molecular interactions of the composition and a melting point wasn't observed, which might be due to the proper incorporation of the SA [17]. Since the MNs must maintain their structural and mechanical stability to be utilised in treating plant diseases, they must penetrate deeply into plant tissue in a minimally intrusive manner [18]. The compression test results are shown in Fig. 4A. The SA-GELMA MNs had practical toughness as there was no discontinuity in the force–displacement curves at approximately 0.45 mm of displacement. The Young's modulus was calculated by keeping the 0.2 strain value constant and dividing the stress value at that point by the strain value. The results showed that GELMA MNs had a young modulus of 35 N/mm, while SA-loaded GELMA MNs had a young modulus of 30 N/mm.

The SA release results are given in Fig. 4B. The SA was detected at 208 nm. During the first 1 h, the burst release behavior was observed, and 37 % of the SA was released, which might be due to leakage of the entrapped SA on the surface of MNs —followed by a slow and controlled release of the SA for up to 24 h, whereas approximately half of the SA was released in 2 h. Erkus et al. observed the amoxicillin release from the GELMA MNs and they found that a 100 % release amount was detected within 48 h [12].

4. Conclusions

GELMA was used to obtain the MNs for plant disease applications. The effect of SA on the morphological properties of the GELMA MNs showed that SA addition did not change the homogeneous geometry of MNs. The compression test results showed that SA addition caused a higher value of compression strength. According to the release test, it can be said that SA was released from the GELMA MNs within 24 h. MNs have a limited drug capacity, leading to concerns about effective dosing, achieving uniform drug distribution across various plant shapes and depths is a challenge, and microneedle durability in changing weather conditions raises questions about long-term effectiveness.

CRediT authorship contribution statement

Ayse Gulcan Ipek: Methodology, Investigation. **Huseyin Berkay Ozarici:** Methodology, Investigation. **Ugur Sayil:** . **Hatice Karabulut:** . **Songul Ulag:** Conceptualization, Methodology, Investigation. **Oguzhan Gunduz:** Conceptualization, Methodology, Investigation.

Declaration of Competing Interest

The authors declare that they have no known competing financial interests or personal relationships that could have appeared to influence the work reported in this paper.

Data availability

Data will be made available on request.

Acknowledgment

This study was supported by TUBITAK (122M906).

References

[1] M.R. Smith, Plants in Industry: Their Role in the Production of Food, Chemicals, and Pharmaceuticals, Cambridge University Press, 2018.
[2] A.C. Velásquez, C.D.M. Castroverde, S.Y. He, Curr Biol. 28 (10) (2018) R619–R634.
[3] G.N. Agrios, Plant Pathology, 6th ed., Academic Press, 2005.
[4] J.B. Jones, T.A. Zitter, M.T. Momol, S.A. Miller, Compendium of Tomato Diseases and Pests, 2nd ed., APS Press, 2013.
[5] E.G. Wulff, J.L. Sørensen, Ann. Rev. Phytopathol. 51 (2013).
[6] S.D. Gittard, J. Agric. Food Chem. 66 (2018) 15.
[7] M.E. Mutlu, S. Ulag, M. Sengor, S. Daglılar, R. Narayan, O. Gunduz, Mater. Lett. 305 (2021).
[8] J. Lee, Mater. Sci. Eng.: C 112 (2020).
[9] V. Alimardani, S.S. Abolmaali, G. Yousefi, Z. Rahiminezhad, M. Abedi, A. Tamaddon, S. Ahadian, J. Clin. Med. 10 (2) (2021) 181.
[10] Z. Luo, W. Sun, J. Fang, K. Lee, S. Li, Z. Gu, M.R. Dokmeci, A. Khademhosseini, Adv. Healthcare Mater. 8 (3) (2019) 1801054.
[11] K. Bialik-Wąs, M. Miastkowska, P. Sapuła, K. Pluta, D. Malina, J. Chwastowski, M. Barczewski, Pharmaceutics 14 (2022) 4.
[12] H. Erkus, T. Bedir, E. Kaya, G.B. Tinaz, O. Gunduz, M.C. Chifiriuc, C.B. Ustundag, Materialia 27 (2023), 101700.
[13] D.F. Fonseca, P.C. Costa, I.F. Almeida, P. Dias-Pereira, L. Correia-Sá, V. Bastos, C. S. Freire, Macromol. Biosci. 20 (10) (2020) 2000195.
[14] Y. Chen, M. Mastalerz, A. Schimmelmann, Internat. J. Coal Geol. 104 (202) (2012) 22–33.
[15] X. Zhou, Z. Luo, A. Baidya, H.J. Kim, C. Wang, X. Jiang, A. Khademhosseini, Adv. Healthcare Mater. 9 (11) (2020) 2000527.
[16] B. Pant, M. Park, G.P. Ojha, D.U. Kim, H.Y. Kim, S.J. Park, Internat. J. Polym. Mater. Polym. Biomater. 67 (12) (2018) 739–744.
[17] N.M. Alotaibi, T. Aouak, Macromol. Res. 21 (2013) 747–756.
[18] H. Karabulut, S. Ulag, B. Dalbayrak, E.D. Arisan, T. Taskin, M.M. Guncu, O. Gunduz, Pharmaceutics 15 (3) (2023) 737.